

# Electronic-controlling nanotribological behavior of textured silicon surfaces fabricated by laser interference lithography

H F Yang, H D He<sup>1</sup>, EL Zhao, J B Hao, J G Qian, W Tang and H Zhu

College of Mechanical & Electrical Engineering, China University of Mining and Technology, XuZhou, 221116, People's Republic of China

E-mail: [hhdcumt@126.com](mailto:hhdcumt@126.com)

Received 30 May 2014, revised 5 June 2014

Accepted for publication 24 July 2014

Published 18 August 2014

## Abstract

The electronic-controlling nanotribological behavior of textured silicon surfaces was investigated by an atomic force microscope (AFM), which were fabricated by laser interference lithography and chemical etching. The results indicated that without an external bias, friction on textured surfaces was greater than that on smooth surfaces and it was related to the coverage rate of the microgrooves. With an external bias, friction on smooth and textured surfaces decreased at first and then increased approximately linearly as the external bias increased.

Keywords: laser interference lithography, micro/nano-texture, electronic controlling, friction

(Some figures may appear in colour only in the online journal)

## 1. Introduction

With the rapid development of the technology, micro/nano-electromechanical systems (M/NEMS) have had a wide range of applications over the last decade due to their excellent performance. As devices in M/NEMS have a large surface area-to-volume ratio, problems caused by friction become more critical. Many studies have confirmed that the usefulness of surface texturing at the micro/nano scale is able to improve the tribological properties of materials [1], but only a few have investigated regular micro/nano-texture, although it is easy to investigate the textures' effect on the friction properties of micro/nano-textured surfaces [2–4]. Various methods, such as ion-beam roughening [5], focused-ion-beam milling (FIB [6, 7]) and current-induced local anodic oxidation [8], have been commonly used to fabricate micro/nano-structures. Laser interference lithography is an attractive method of fabricating periodical micro-/nano-structures over a large area. It is maskless, effective, fast and low cost and only needs a few minutes' exposure and development [9, 10].

In M/NEMS, some devices have to work under an external electric field. Hence, it is promising to ascertain the relation

between frictional properties and an external electric field in micro-/nanotribology. AFM is an ideal tool for studying tribological properties at micro/nano scale. The University of California has discussed the frictional behaviors of materials under an external electric field. In 2006, they published a paper discussing electronic controlling of friction in silicon pn junctions in *Science* [11]. In 2008 [12], using a Pt-coated tip with a 50 nm radius in an AFM sliding against an n-type GaAs(100) substrate, they investigated the electronic contribution to friction on semiconductor surfaces, which were covered by an approximately 1 nm oxide layer. They observed a substantial increase in friction force in accumulation (forward bias) with respect to depletion (reverse bias). In 2010, they found the correlations between charge transport and nano mechanical properties on organic molecular films probed with AFM. In addition, they addressed the role of molecular deformation and bending in friction and conductance measurement [13].

However, there have been few investigations focusing on the influence of an external electric field on the tribological performance of regular micro-textured surfaces. In the present study, silicon surfaces patterned with microgrooves of different pitch were fabricated by laser interference lithography and chemical etching [14] and their electronic tribological behavior was systematically investigated by an AFM.

<sup>1</sup> Author to whom any correspondence should be addressed.

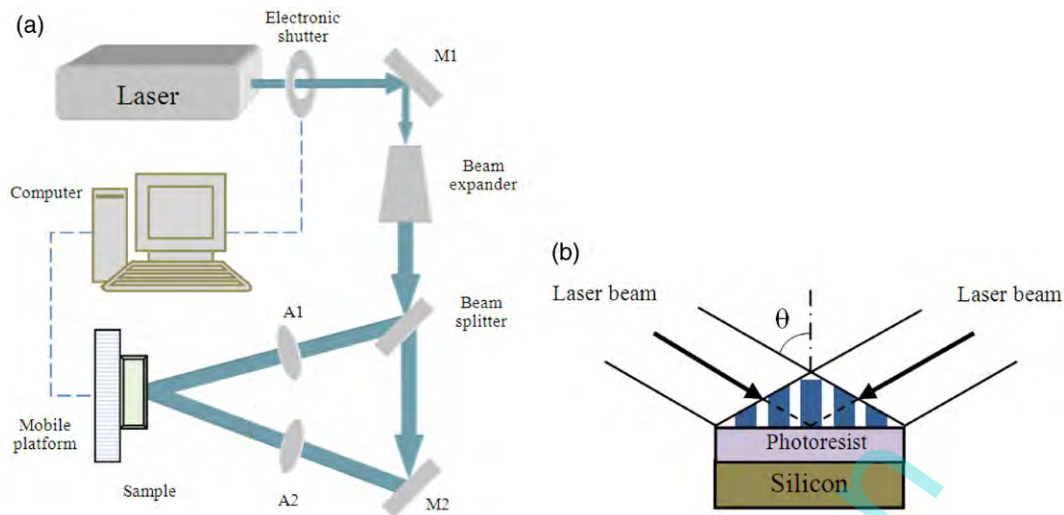


**Figure 1.** (a) Optical layout of laser interference lithography. A: attenuator, M: mirror. (b) Two-beam laser interference.

## 2. Experimental details

The research applied laser interference lithography to the fabrication of microgrooves, which was shown schematically in figure 1(a). An ultraviolet laser (DSH-355-10, PHOTONICS INDUSTRIES, USA) operating at a wavelength of 355 nm was served as the exposure source and an electronic shutter was used to control the exposure time. The laser beam was completely reflected by a mirror (M1). The laser beam was filtered and expanded by a beam expander, which was composed of two lenses and a pinhole. The beam expander allowed the high-frequency noise to be removed from the laser beam to provide a clean Gaussian profile. An optical beam splitter divided the laser beam into two coherent parts—one was reflected and the other was transmitted and guided by a mirror (M2). The attenuators ensured that both beams were at equal power. The period of interference patterns could be easily changed by adjusting the half-angle of the two beams' intersect angle ( $\theta$ ), as shown in figure 1(b).

N-type single-crystal silicon (100) was cut to the size of  $1.5 \times 1.5 \text{ cm}^2$ . After ultrasonic cleaning by acetone, absolute alcohol and deionized water for 5 min, respectively, positive photoresist (BP212-37) was spin-coated onto the polished surface of a substrate at speeds of 500 rpm for 30 s and 5,000 rpm for 60 s. Then it was baked in a drying oven at  $90^\circ\text{C}$  for 20 min, according to the manufacturer's specifications. The microgrooves pattern was recorded on the photo resist by a few seconds' exposure (for a dose of  $60\text{--}70 \text{ mJ cm}^{-2}$ ) in the system of laser interference lithography shown in figure 1(a). After that, the sample was developed in the positive photo resist developer (KMP PD238-II) for 15 s to achieve microgrooves, followed by hardening at  $120^\circ\text{C}$  for an hour. The photo resist pattern was transferred to silicon by wet chemical etching. The etching liquid was a mixture solution of  $\text{HNO}_3(65\text{--}68\%): \text{HF}(40\%): \text{H}_2\text{O} = 2:1:1$ . Finally, the sample was immersed in positive photo resist stripper (KMP ST600) for 30 min in order to remove the residual photo resist.

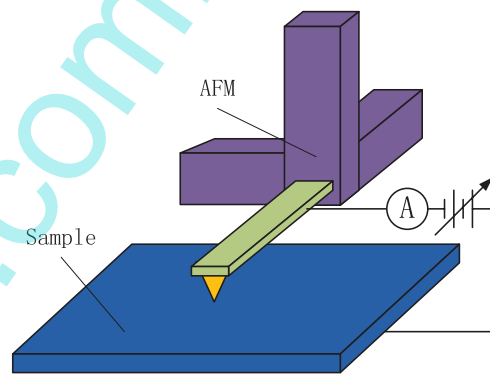


**Figure 2.** Schematic of AFM measurement of electronic controlled friction.

The friction experiments were characterized by AFM/FFM (CSPM5500 electronics, Ben Yuan Nano-Instrument, China) using the CAFM mode. The nominal spring constant of the cantilevers was  $0.2 \text{ N m}^{-1}$  and the resonant frequency was 13 kHz. The probe was coated with a conducting layer of Au film. A voltage was applied between the sample and tip, as shown in figure 2. Friction measurements were performed at a scanning rate of 1 Hz and a scanning length of  $30.0 \mu\text{m}$ , under applied normal loads in the range of 0.1–1.0 V with bias voltage of 0.0 V, 0.5 V, 1.0 V, 1.5 V and 2.0 V, respectively. All the tests were conducted at room temperature and relative humidity of 30%.

## 3. Results and discussion

### 3.1. Characterization of surface-textured silicon

Figure 3 shows 2D, 3D and line section AFM images of microgrooves on patterned silicon surfaces with different pitches of  $3.2 \mu\text{m}$ ,  $3.7 \mu\text{m}$ ,  $5.8 \mu\text{m}$  and  $8.6 \mu\text{m}$ , ascribed as S1, S2, S3 and S4, respectively. Microgrooves with various pitches were fabricated in the system shown in figure 1(a) through adjusting  $\theta$ . The interference period can be calculated from  $P = \lambda/2\sin\theta$ , where

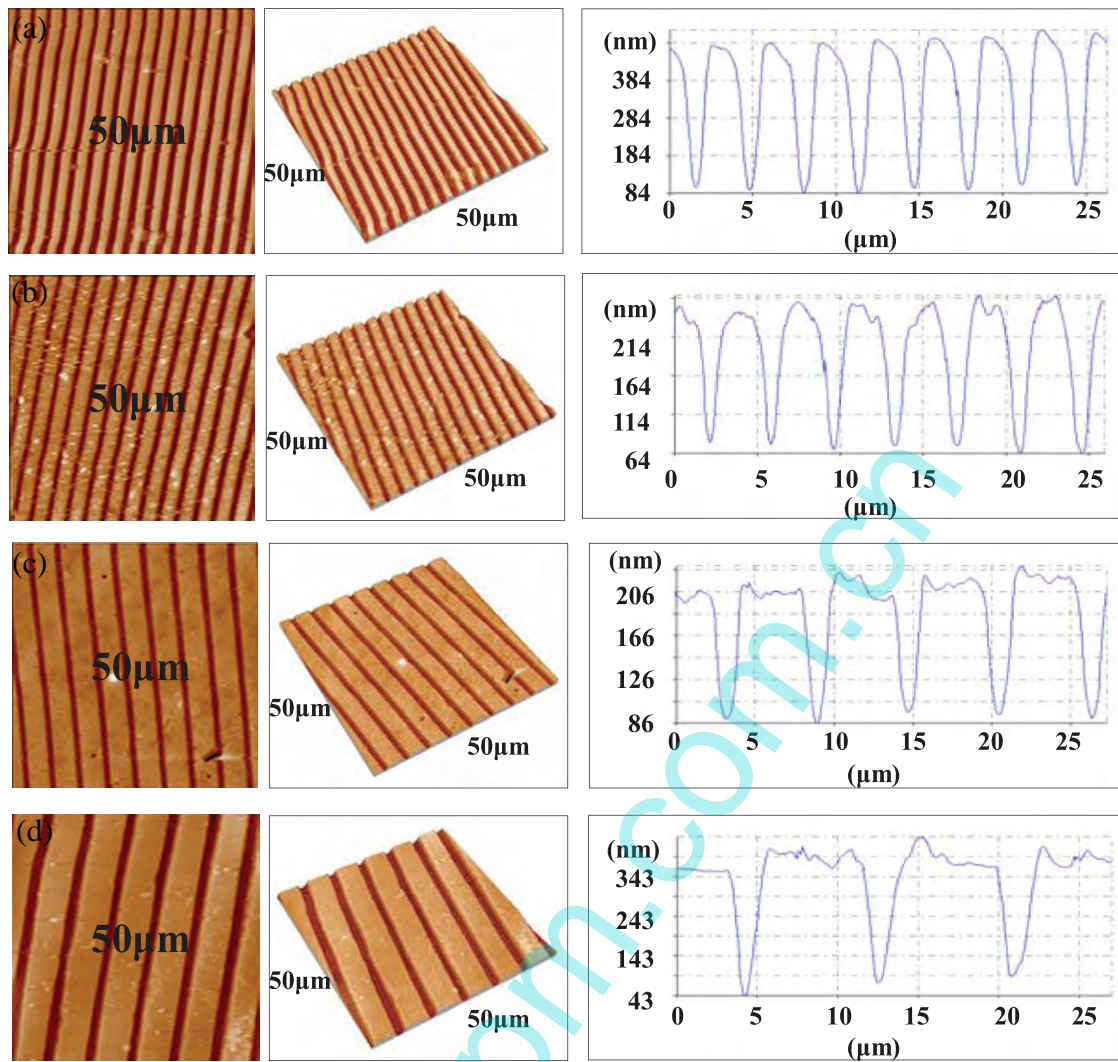


**Figure 3.** 2D, 3D and line cross profile analysis AFM topographic images of the patterned silicon surfaces with different pitches. (a) 3.2 μm; (b) 3.7 μm; (c) 5.8 μm; (d) 8.6 μm.

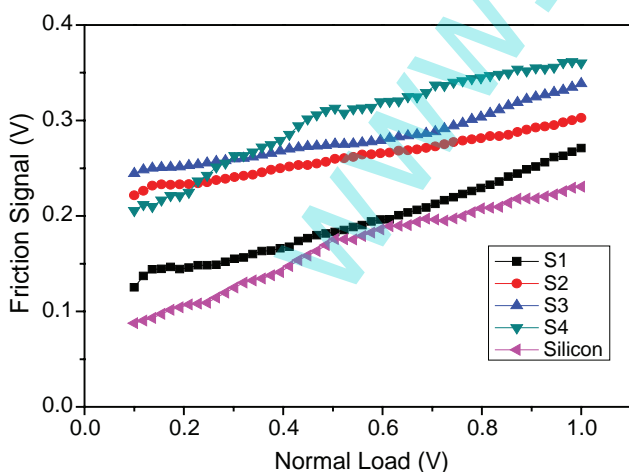


**Figure 4.** Plots of friction force versus load curves for the textured surfaces with different pitches and smooth silicon.

$\lambda$  is the wavelength of the laser beams. It was obvious that the microgrooves fabricated by laser interference lithography and chemical etching were regular and the cliff of them was smooth.

**Table 1.** Geometrical parameters of patterned silicon surfaces with microgrooves.

Sample	Pitch ( $\mu\text{m}$ )	Space width (nm)	R (%)
S1 S2	3.2 3.7	979 1017	30.1 27.5
S3	5.8	1224	21.1
S4	8.6	1078	12.5

### 3.2. Nanofriction properties

(1) Without an external field. Figure 4 shows the average ‘friction force versus load’ curves for S1, S2, S3, S4 and smooth silicon, wherein each data point was an average of 5 times experiments. It was obvious that the friction force increased as normal load increased for each sample and the friction force of textured surfaces was greater than that of smooth surface. When normal load exceeded 0.3 V, the friction force of textured surfaces grew as the pitch of microgrooves increased.

At nanoscale, the real area of contact strongly affects friction, according to the fundamental law of friction given

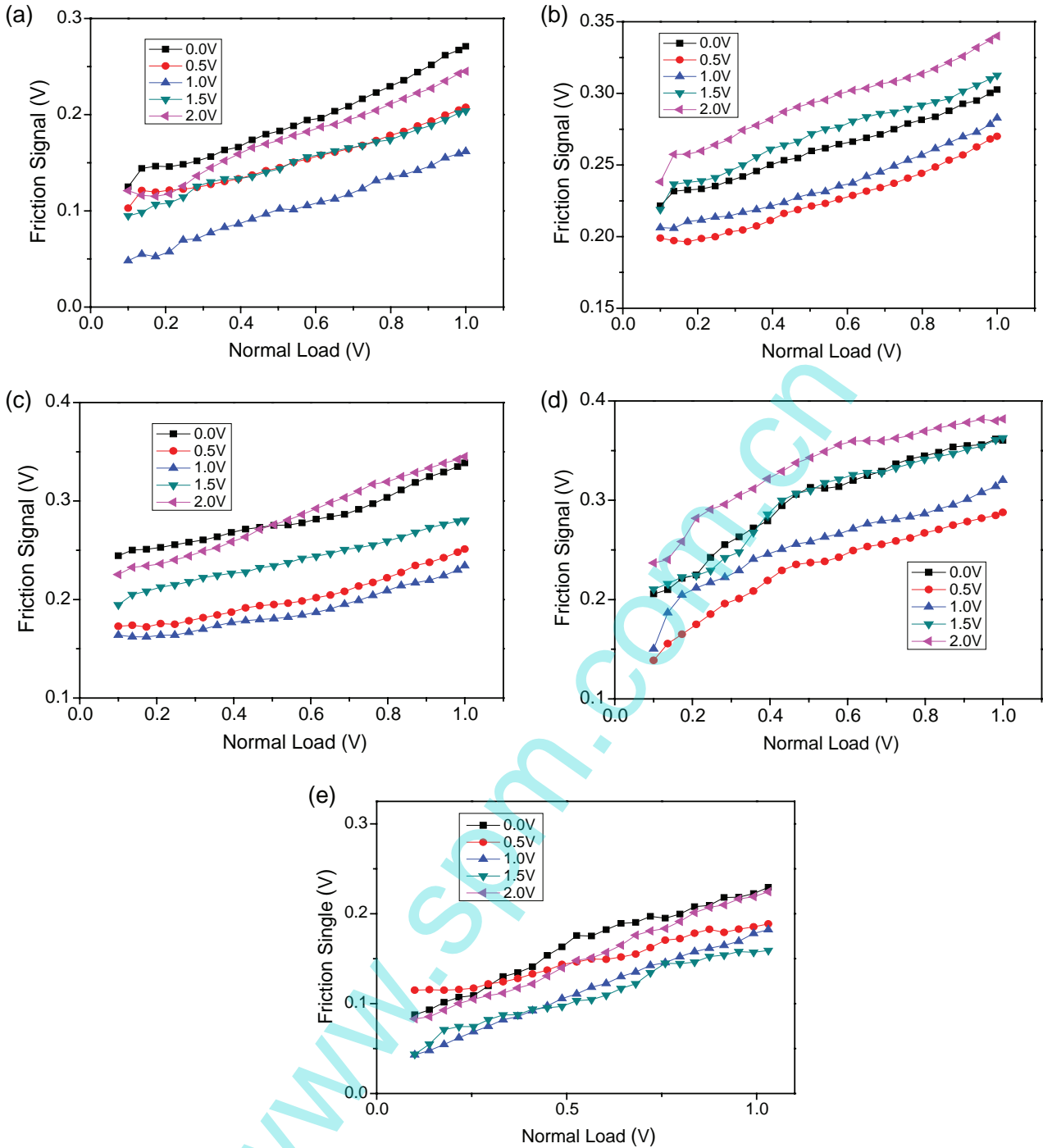


**Figure 5.** Plot of the friction force as a function of bias with the normal load from 0.1 V to 1.0V.

by Bowden and Tabor that  $F_f = \tau A_r$ , where  $\tau$  is the shear strength, an interfacial property related to Young’s modulus and Poisson’s ratio.  $A_r$  is the real area of contact [15]. As the normal load increased, the contact area of the tip and silicon surfaces increased because of stress deformation. Wang [2] and Zhao [4] thought the real area of contact was mainly determined by the micro/nano-texture fractional surface coverage of material surfaces. With increased fractional surface coverage of micro/nano grooves, the number of asperities in contact reduced, which decreased the real area of contact and led to a lower friction force. The geometrical parameters

of microgrooves for S1, S2, S3 and S4 are listed in table 1.  $R(\%)$  stands for the microgrooves’ fractional surface coverage, which is calculated from  $R(\%) = NS_{space}/S_{scan} = NW/a$ . Here,  $N$  refers to the number of grooves;  $S_{space}$  and  $S_{scan}$  are the area of a space and the patterned surface, respectively;  $W$  is the space width of a microgroove;  $a$  is the length of the patterned surface perpendicular to the direction of the microgrooves. As seen in table 1, the microgrooves’ fractional surface coverage was 30.1%, 27.5%, 21.1% and 12.5% from S1 to S4. The contact area increased from low to high, according to the papers presented by Wang and Zhao. Thus, the results in figure 4 were

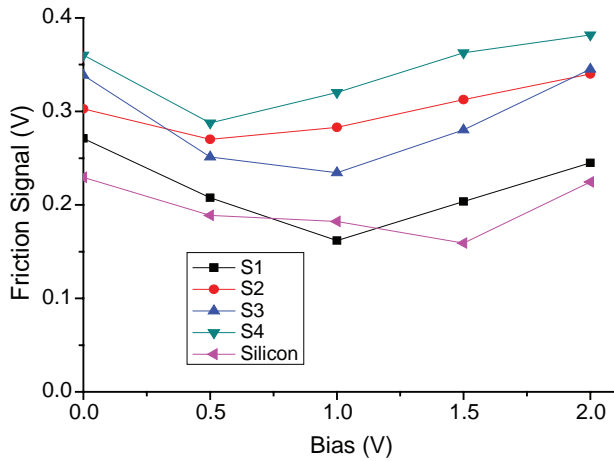


**Figure 6.** Plot of the friction force as a function of bias with the constant normal load of 1.0V.

agreed with the conclusion presented by Wang and Zhao that friction of the microgroove-patterned surfaces decreased as the microgrooves' fractional surface coverage increased, due to the diminution of the contact area. In addition, the reduction of friction was also related to the real sliding velocity. Thompson [16] and Robbins [17] presented that the total friction efficiency decreased with the increase of sliding velocity, according to computer simulations. Nikhil [18] found that the friction force decreased with the increase of velocity when the tip-scanning velocity exceeded a certain critical velocity. During the experiments, sliding velocity was invariable, the direction of which was horizontal. When the textured surfaces were tested, the real sliding velocity was resultant velocity from horizontal and vertical velocity. With increased fractional surface coverage of textures, the average of real sliding velocity was increased, leading to reduction of friction force.

(2) With an external field. Figure 5 showed the friction force for S1, S2, S3, S4 and smooth silicon versus load from 0.1V to 1V at a bias of 0.0V, 0.5V, 1.0V, 1.5V and 2.0V, respectively. It was clearly implied that friction force was able to be controlled by an external electric field, which changed with the value of external bias. With an external field, the friction force still increased as normal load increased for each sample. Figure 6 showed the friction force versus bias at the constant normal load of 1.0V for S1, S2, S3, S4 and smooth silicon. The results indicated that the friction force decreased with the increase of external bias firstly and then increased approximately linearly. Friction force could be controlled by an external field. Through controlling the value of external bias, friction force could be increased or decreased and it was at minimum when external bias was nearly 0.5V and 1.0V.

With an external electric field, the voltages on the tip and silicon surfaces were opposite each other, as shown in figure 2, which generated electrical attraction. The attractive force acted as a part of the normal load. During the repeated relative movement of the tip and silicon surfaces, the friction pair of Au/Si would generate [19, 20] voltage  $V_s$ , the direction

of which might be contrary to the external electric voltage, defined as  $V_e$ . Thus, the real value of bias  $V_r$ , loaded between the tip and silicon surfaces could be calculated from  $V_r = V_e - V_s$ . When the value of  $V_e$  was less than  $V_s$ ,  $V_r$  decreased as  $V_e$  increased, leading to reduction of friction force. As the value of  $V_e$  was more than  $V_s$ , friction force would increase with  $V_e$ , because of the increasing of electric attractive force.

#### 4. Conclusion

Microgrooves with various pitches were created on silicon surfaces by means of laser interference and chemical etching. The effect of surface textures on the frictional properties of silicon surfaces and the nano tribological behavior with an external electric field were investigated by an AFM. Conclusions drawn from this work are as follows:

1. The friction force of microgroove-patterned silicon surfaces without an external electric field decreased with the increase of the microgroove fractional surface coverage, which could be controlled by the pitch of the microgrooves.
2. During the repeated relative movement of the tip and silicon surfaces, the friction pair of Au/Si would generate voltage, the direction of which was contrary to the external electric voltage. The real value of bias between the Au tip and silicon sample decreased with the increase of bias when the value of bias was below the value of self-generated voltage. When the value of bias was above the value of self-generated voltage, the real value of bias increased with the increase of bias. Thus, the friction force of the Au/Si friction pair decreased with the increase of bias loaded between the tip and silicon surfaces firstly and then increased.

#### Acknowledgments

The author gratefully acknowledges the Natural Science Foundation of China (NSFC 51105360), the Natural Science Foundation of Jiangsu province (BK2011218), and the Fundamental Research Funds for the Central Universities under Grant (2012QNA25) for supporting this work.

#### References

- [1] Etsion I 2005 State of the art in laser surface texturing *J. Tribol. Trans. ASME* **127** 248–53
- [2] Wang Y, Wang L, Xue Q, Yuan N and Ding J 2010 A facile method to improve tribological properties of silicon surface by combining nanogrooves patterning and thin film lubrication *Colloids Surf. A: Physicochem. Eng. Asp.* **372** 139–45
- [3] Zhang X, Lu Y, Liu E, Yi G and Jia J 2012 Adhesion and friction studies of microsphere-patterned surfaces in contact with atomic force microscopy colloidal probe *Colloids Surf. A: Physicochem. Eng. Asp.* **401** 90–6
- [4] Zhao W, Wang L and Xue Q 2010 Colloids and Influence of micro/nano-textures and chemical modification on the nano tribological property of an surface *Colloids Surf. A: Physicochem. Eng. Asp.* **366** 191–6

- [5] Yoon E S, Yang S H, Kong H and Kim K H 2003 The effect of topography on water wetting and micro/nano tribological characteristics of polymeric surfaces *Tribol. Lett.* **15** 145–54
- [6] Ando Y, Tanaka T, Ino J and Kakuta K 2001 Relationships of friction, pull-off forces and nanometer-scale surface geometry *JSME Int. J. Ser. C* **44** 453–61
- [7] Ando Y 2000 The effect of relative humidity on friction and pull-off forces measured on submicron-size asperity arrays *Wear* **238** 12–9
- [8] Mo Y, Zhao W, Huang D, Zhao F and Bai M 2009 Nanotribological properties of precision-controlled regular nanotexture on H-passivated Si surface by current-induced local anodic oxidation *Ultramicroscopy* **109** 247–52
- [9] Yang Y-L, Hsu C-C, Chang T-L, Kuo L-S and Chen P-H 2010 Study on wetting properties of periodical nano patterns by a combinative technique of photolithography and laser interference lithography *Appl. Surf. Sci.* **256** 3683–7
- [10] Rodriguez A et al 2009 Laser interference lithography for nanoscale structuring of materials: from laboratory to industry *Microelectron. Eng.* **86** 937–40
- [11] Park J Y, Ogletree D F, Thiel P A and Salmeron M 2006 Electronic control of friction in silicon pn junctions *Science* **313** 186
- [12] Qi Y, Park J Y and Hendriksen B L M 2008 Electronic contribution to friction on GaAs: an atomic force microscope study *Phys. Rev. B* **77** 184105
- [13] Park J Y and Qi Y 2010 Probing nanotribological and electrical properties of organic molecular films with atomic force microscopy *Scanning* **32** 257–64
- [14] Zhang J and Meng Y 2012 A study of surface texturing of carbon steel by photochemical machining *J. Mater. Process. Technol.* **212** 2133–40
- [15] Yifei M, Turner K T and Szlufarska I 2009 Friction laws at the nanoscale *Nature* **457** 1116–9
- [16] Tambe N S and Bhushan B 2005 Nanoscale friction-induced phase transformation of diamond-like carbon *Scripta Materialia* **52** 751–5
- [17] Robbins M O and Thompson P A 1991 Critical velocity of stick-slip motion *Science* **253** 916
- [18] Thompson P A and Robbins M O 1990 Origin of stick-slip motion in boundary lubrication *Science* **250** 792–4
- [19] Zhai W and Qi Y 2001 Effects of metallic surface film and wear debris on the dry sliding behavior and self-generated voltage of various metal-metal systems *Tribology* **21** 70–2
- [20] Ao H, Gao Y, Zhai W and Qi Y 1999 An experimental research on self-generated potential of ball-disc friction pair under normal pressure and low and middle vacuum *Tribology* **19** 250–4